Supplementary Information

Active Tumor Targeting by Core-Shell PDMS-HA Nanoparticles with Sequential Delivery of Doxorubicin and Quercetin to overcome P-glycoprotein efflux pump

Madhu Verma[a,b], Krishna Yadav[c], Rashmi Parihar[c], Debjani Dutta[b]*, Surabhi Chaudhuri[b]* and Sri Sivakumar[a,d,e*]

[a]Department of Chemical Engineering, Indian Institute of Technology Kanpur, Kanpur, Uttar Pradesh, India

[b]Department of Biotechnology, National Institute of Technology Durgapur, Durgapur, West Bengal, India

[c] Central Experimental Animal Facility, Indian Institute of Technology Kanpur, Kanpur, Uttar Pradesh, India

[d]Material Science Programme, Indian Institute of Technology Kanpur, Kanpur, Uttar Pradesh, India

[e]Centre for Environmental Science and Engineering, Center for Nanosciences, Mehta Family Centre for Engineering in Medicine, Gangwal School of Medical Sciences and Technology Indian Institute of Technology Kanpur, Kanpur, Uttar Pradesh, India

Table S1. NPs-based phytochemical-chemotherapeutic combination therapy for different cancer models.

Phyto-chemical	Chemo-therapeutic Drug	Drug Delivery System (DDS)	Observations	Cancer model	Ref.
Curcumin	Cisplatin	Co-encapsulatuion in Layer-by-layer NPs	Co-encapsulated NPs minimize blood Cis-Pt and curcumin degradation and boost tumor drug accumulation.	Lung cancer	1
Quercetin	Paclitaxel	Mesoporous Silica	Successfully overcome the drug resistance and enhanced antitumor activity	Breast cancer	2
Curcumin	Adriamycin	Co-encapsulation and Ph-sensitive	The prolonged release of PH-responsive U11-DOX/curcumin NPs has a high synergistic impact.	Lung cancer	3

EGCG	5-FU	Gelatin and chitosan NPs Co-encapsulated	Anti-tumor efficacy, high absorption, and enhanced circulation time.	Colorectal cancer	4
Resveratrol	Oxaliplatin	N, O-carboxymethyl chitosan NPs	The combination had much higher anti-cancer action compared to free drug	Colorectal cancer	5
Epigallocatechin Gallate	Doxorubicin	HA-PEG-gelatin NPs	The combination effectively reduces tumor and offers cardioprotective activity	Gastric Cancer	6
Curcumin	Doxorubicin	Chitosan-cystamine-PCL copolymer micelle with glycyrrhetinic acid.	Improve micelle uptake by cells and enhance anti-tumor effects.	Hepatocellular carcinoma	7
Resveratrol	Paclitaxel	Co-encapsulated and PEGylated liposome	Effectively reverse resistant to chemotherapy- cancer cells	Breast cancer	8
Curcumin	Methotrexate	Co-encapsulated in PLGA NPs	Shows the synergistic impact of co-delivering methotrexate and curcumin in impeding the advancement of breast cancer.	Breast cancer	9
Quercetin	Tamoxifen	Co-encapsulated in PLGA NPs	Enhanced bioavailability, improved effectiveness, and decreased toxicity	Breast cancer	10
Betulinic acid	Gemcitabine	PLGA-PEG NPs, Co-encapsulated	The efficacy of this combination in suppressing solid tumor models is higher.	Pancreatic cancer	11
Quercetin	Doxorubicin	Polymeric Micelles	High loading and anti-tumor activity	Liver cancer	12

Table S2. Sample codes and their abbreviations.

S. No.	Sample codes	Abbreviations
1.	SCMS Silica NPs	Solid Core Mesoporous Shell Silica Nanoparticles
2.	PDMS NPs	Polydimethylsiloxane Nanoparticles
3.	PDMS-HA NPs	Core-Shell Polydimethylsiloxane Nanoparticles with Hyaluronic Acid Modification
4.	Que- PDMS-HA NPs	Quercetin loaded Core-Shell Polydimethylsiloxane Nanoparticles with Hyaluronic Acid Modification
5.	Dox- PDMS-HA NPs	Doxorubicin loaded Core-Shell Polydimethylsiloxane Nanoparticles with Hyaluronic Acid Modification
6.	Que-Dox-PDMS-HA NPs	Quercetin and Doxorubicin loaded Core-Shell Polydimethylsiloxane Nanoparticles with Hyaluronic Acid Modification

Results

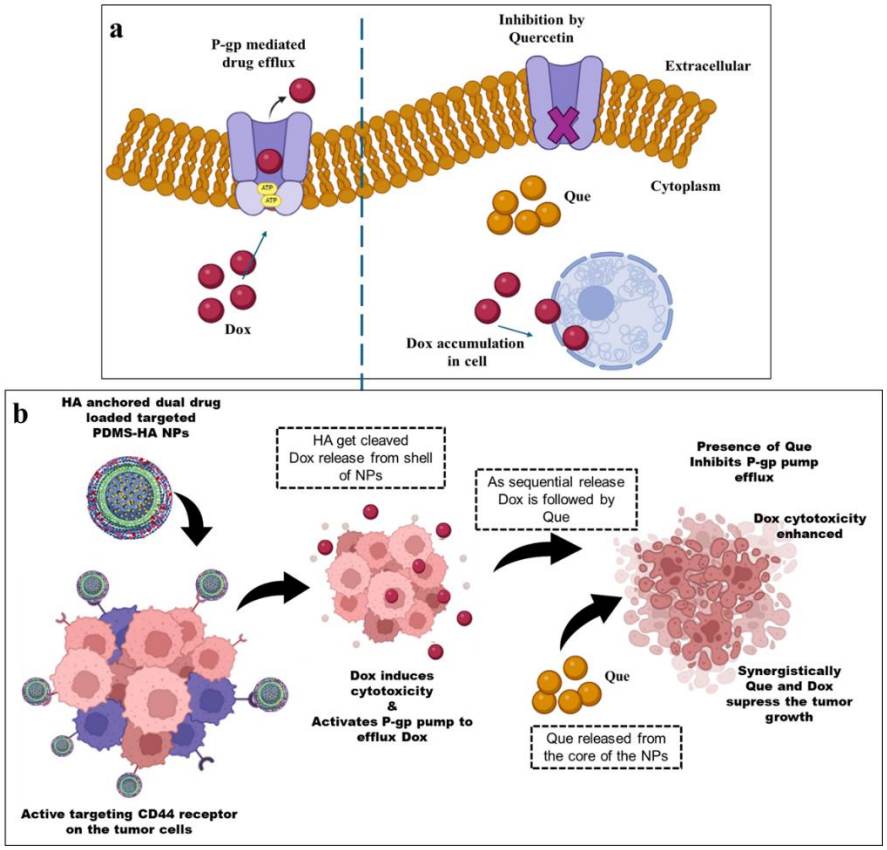

Scheme S1. (A) multi drug resistance (MDR) mechanism by P-gp efflux pump and quercetin inhibitory effect. (B) The sequential release of Dox and Que from PDMS-HA NPs contributes to suppress the tumor growth.

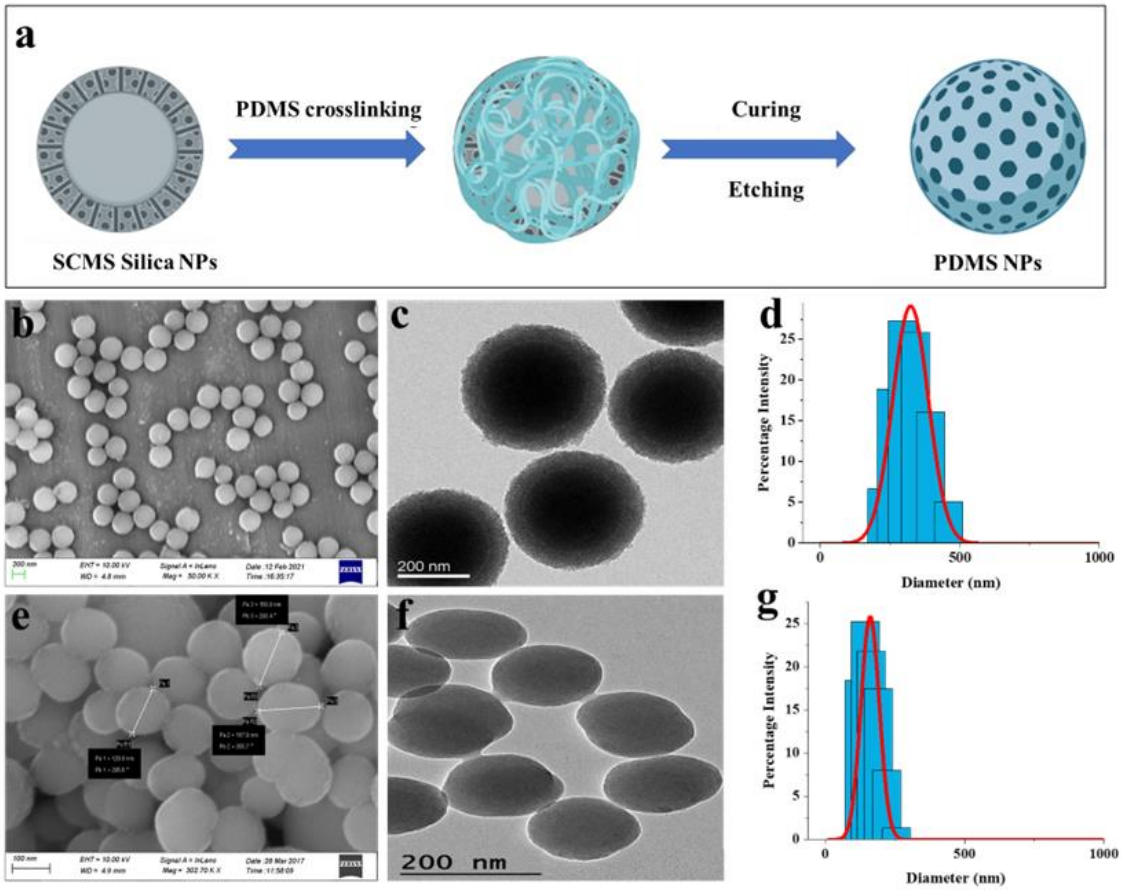

Fig. S1 Fabrication and characterization of SCMS silica NPs and PDMS NPs (a) Synthesis scheme, (b) SEM images, (c) TEM image, and (d) DLS graph of SCMS Silica NPs used as a template. (e) SEM, (f) TEM, and (g) DLS graph for bare PDMS NPs.

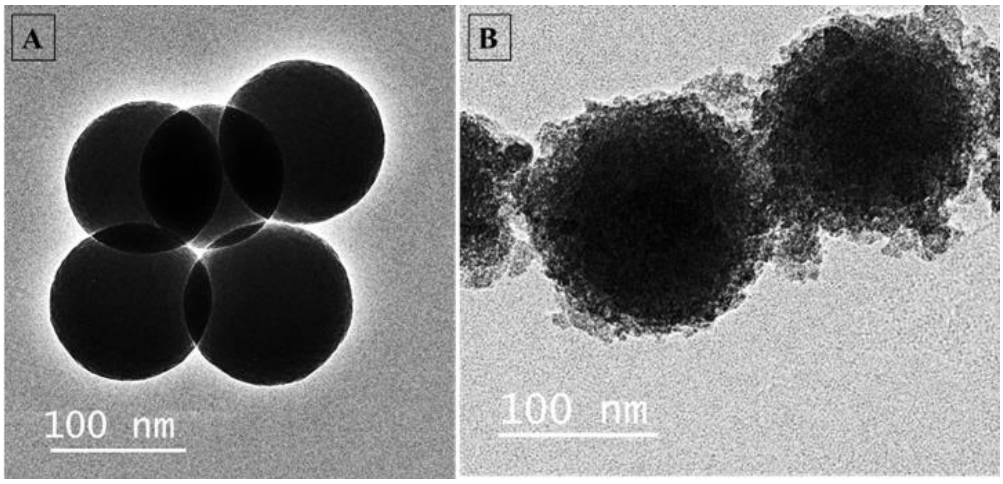

Fig. S2 TEM images (a) Que-PDMS NPs and (b) Que- PDMS-PEI NPs.

a

Samples	DLS (d.nm)	PDI	Std dev (nm)
Silica NPs	283.7	0.11	9.3
PDMS NPs	165.5	0.18	12.6
Que-PDMS NPs	168.8	0.21	11.4
PDMS- PEI NPs	179.5	0.26	14.7
Que-PDMS-PEI- NPs	182.3	0.23	8.2
PDMS-PEI-HA NPs	206.2	0.29	18.5
Que-Dox-PDMS-PEI-HA NPs	211.2	0.26	12.2

b

Samples	Zeta Potential (mV)	Std. Dev (mV)
Silica NPs	-43.4	5.9
PDMS NPs	-41.7	5.4
Que-PDMS NPs	-48.2	8.3
PDMS- PEI NPs	31.5	3.5
Que-PDMS-PEI NPs	29.6	4.1
PDMS-PEI-HA NPs	-37.6	6.3
Que-Dox-PDMS-PEI-HA NPs	35.4	5.2

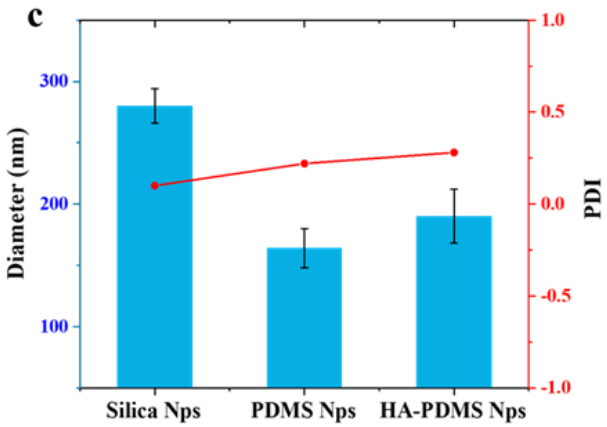

Fig. S3 DLS analysis (a, c) and Zeta potential (b) of SCMS silica NPs, PDMS NPs, PDMS-HA NPs and loaded nanoformulations. Each point represents the mean ± SE (n = 3).

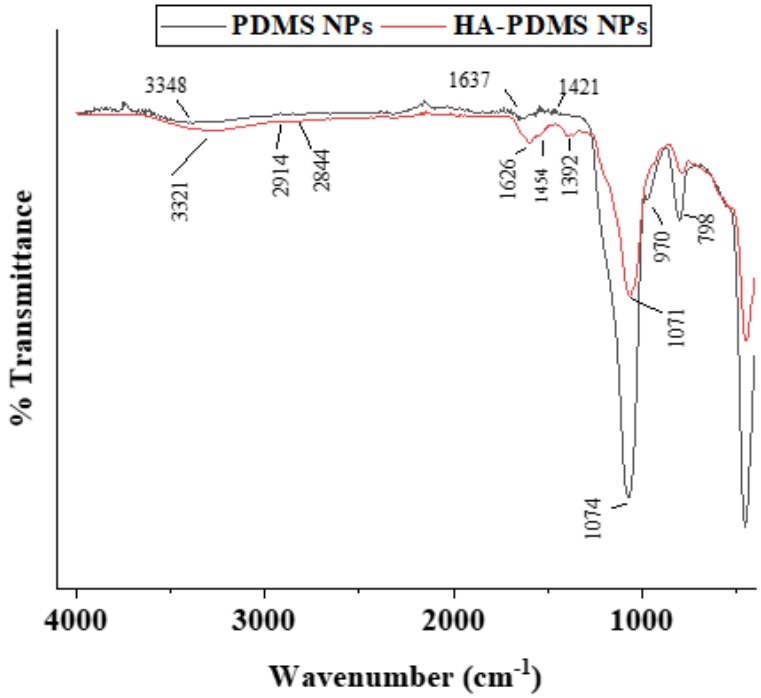

Fig.S4 FTIR spectra for PDMS NPs and PDMS-HA NPs.

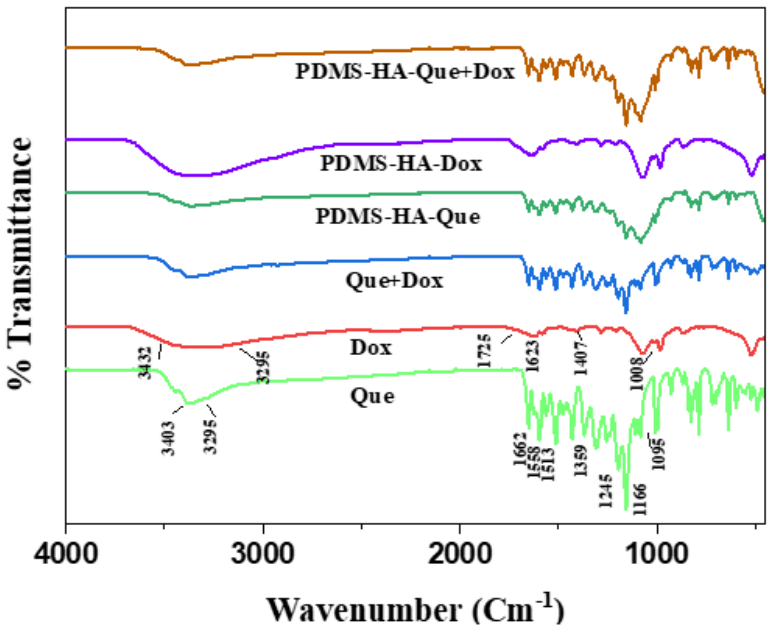

Fig.S5 FTIR spectra for Que, Dox, and Que-Dox-PDMS-HA NPs.

Table S3. FTIR spectrum of PDMS-HA NPs

Transmittance Peaks (cm^{-1})	**Functional Group**
-874	Si-CH_3
- 1078	Si-O-Si
- 970	=C-H
- 1251	Si-CH_3
-1626	C=C
1617, 1409	C=0
-2988	-CH_3
-3568	OH stretch

Table S4. FTIR spectrum of quercetin and doxorubicin.

Transmittance Peaks (cm^{-1})	**Functional Group**
1200–1300	C-O stretching
1500–1600	C=C stretching
1650–1700	C=O stretching
3200–3500	OH stretch
-3318.02	O-H and N-H stretch

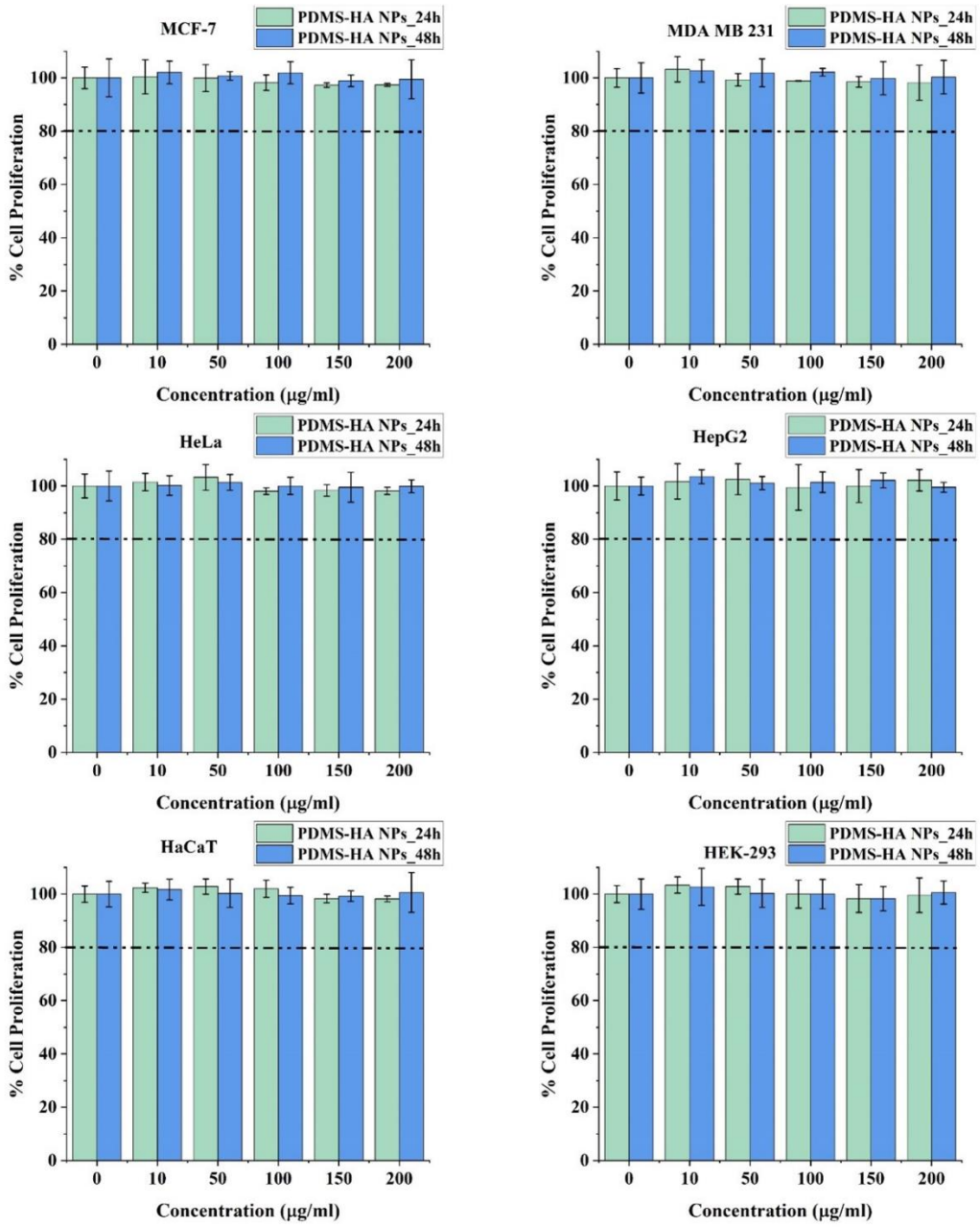

Fig. S6 MTT assay at different concentrations of PDMS-HA NPs (10, 50, 100, 150 and 200 µg/ml) with MCF-7, MDA-MB-231, HeLa, HepG2, HaCaT and HEK-293 cell lines for 24 and 48 hours. Each point represents the mean ± SE (n = 3).

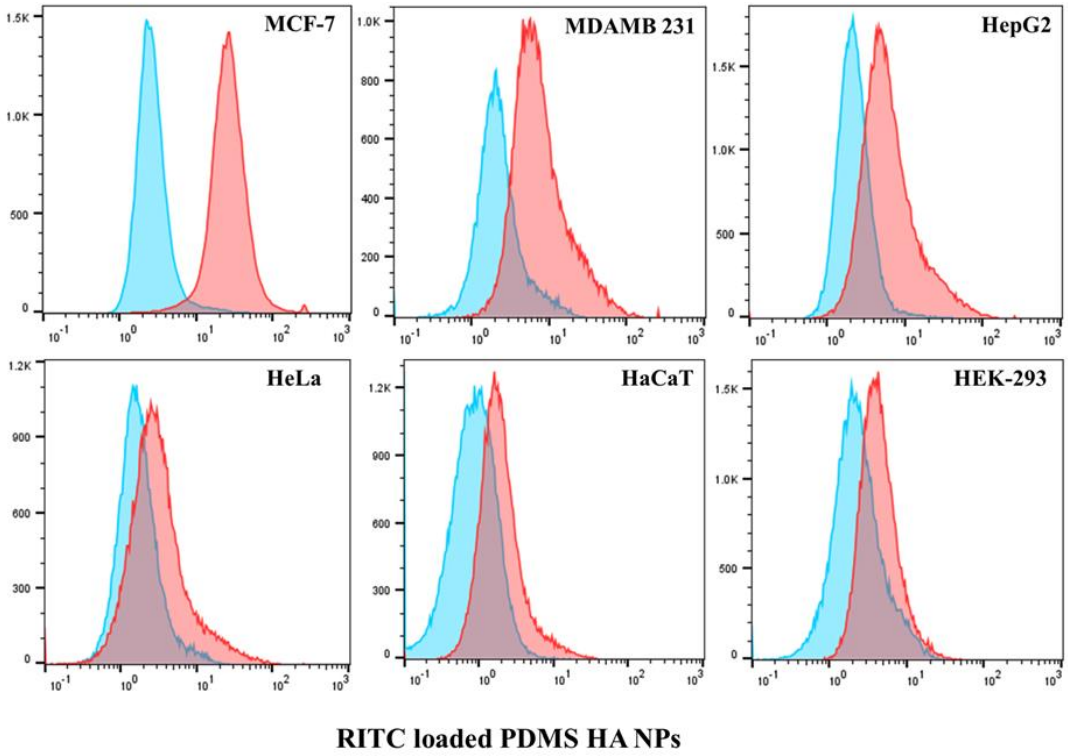

Fig. S7 Uptake studies of RITC-PDMS-HA NPs (100 µg/ml) with MCF-7, MDA-MB-231, HeLa, HepG2, HaCaT, and HEK-293 cell lines by using flow cytometry.

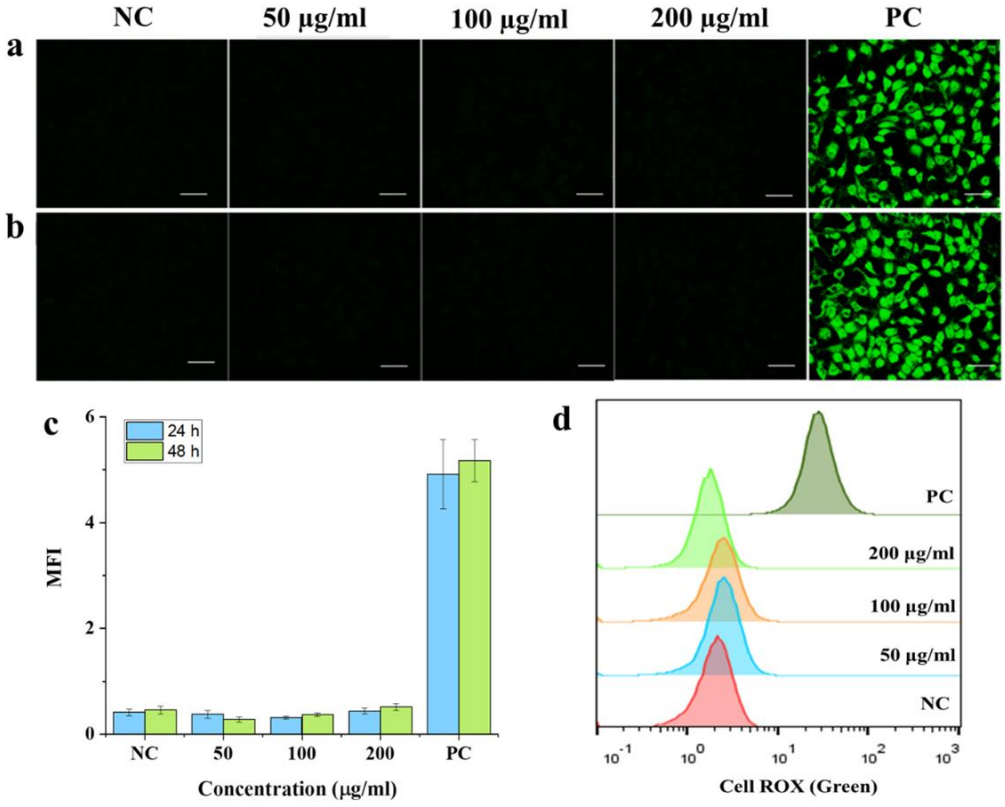

Fig. S8 ROS studies with DCFDA for PDMS-HA NPs at concentrations of PDMS-HA NPs (50, 100, 200 µg/ml) for (a) 24, and (b) 48 h on MCF-7 cell lines. NC (Negative control,

untreated cells) and PC (Positive control, H_2O_2 treated cells). (c) MFI for 24 and 48 h treatments. (d) flow cytometry analysis for ROS generation by Cell-ROX. Scale bar 20µm.

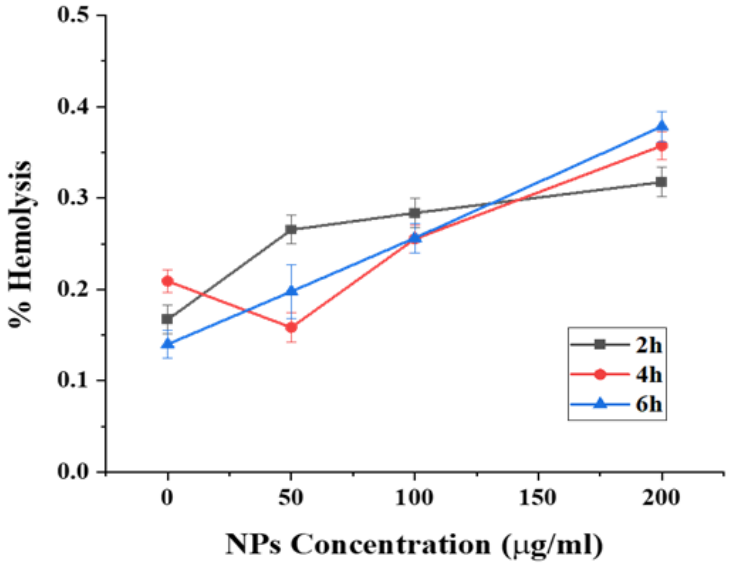

Fig. S9 Hemolysis assay for PDMS-HA Nps for 2h, 4h, and 6h at concentrations (50, 100, 200 µg/ml). Negative control (PBS) and Positive control (Triton X). The quantity of hemoglobin released from the red blood cells was assessed by measuring the absorbance of the supernatant.

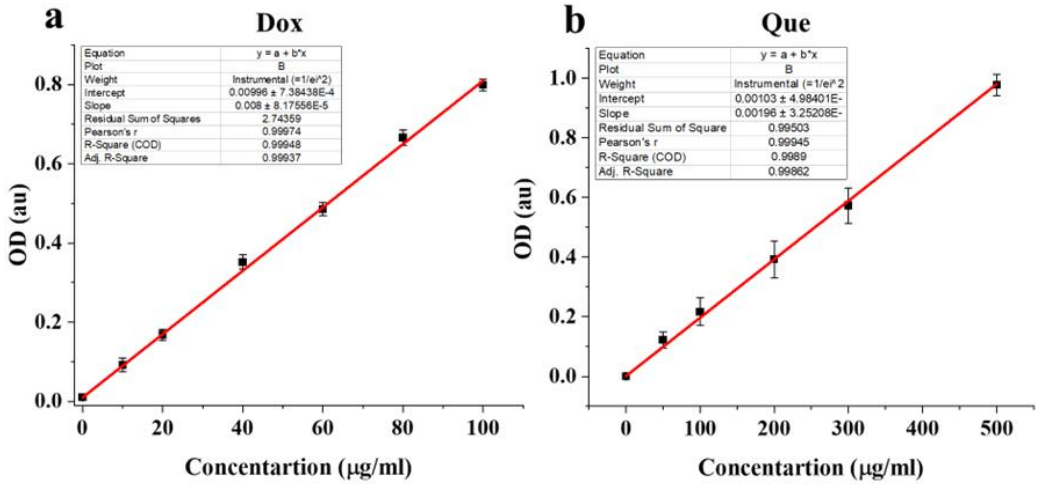

Fig. S10 Calibration curves (a) Dox absorbance at 485 nm. (b) Que absorbance at 415 nm. Each point represents the mean ± SE (n = 3).

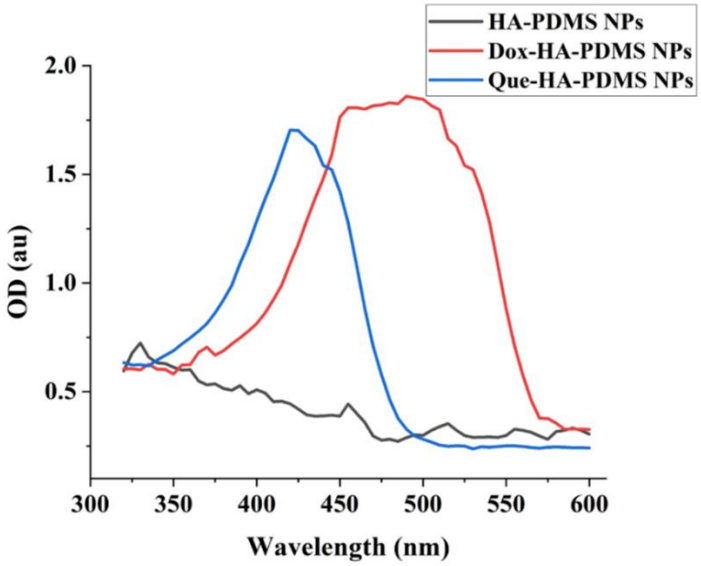

Fig. S11 UV-Visible absorption spectra for loading of Que and Dox on PDMS-HA NPs.

Table S5. Details of the amount of Que and Dox loaded on PDMS-HA NPs used for the cytotoxicity assay.

PDMS-HA NPs	**Que**		**Dox**	
(µg/ml)	**(µg/ml)**	**(µM)**	**(µg/ml)**	**(µM)**
5	1.05	3.10	0.31	0.52
10	2.10	6.20	0.62	1.05
25	5.25	15.52	1.50	2.63
50	10.50	31.04	3.10	5.26
100	21.00	62.08	6.20	10.52
200	42.00	124.16	12.40	20.71

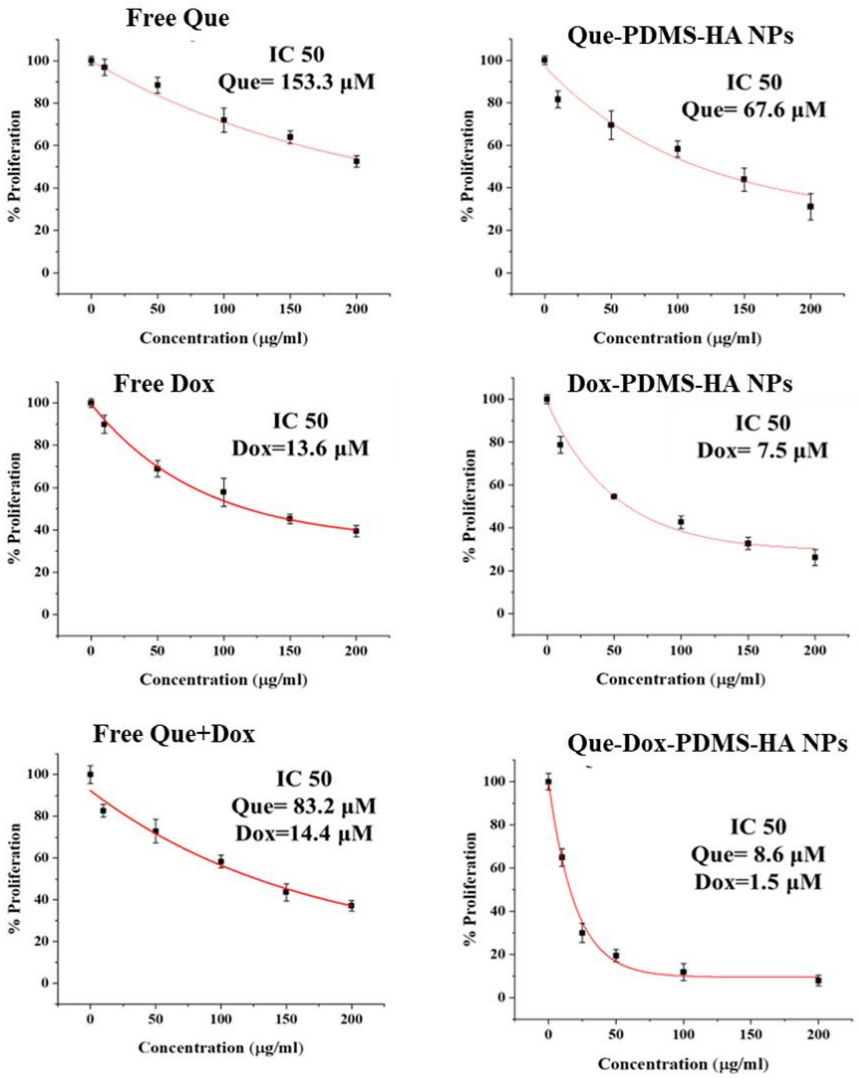

Fig. S12 IC50 fitting curve of free Que, free Dox, free Que+Dox, Que-PDMS-HA NPs, Dox-PDMS-HA NPs, and Que-Dox-PDMS-HA NPs for MCF-7 cells. Each data point signifies the average ± standard error (n = 3).

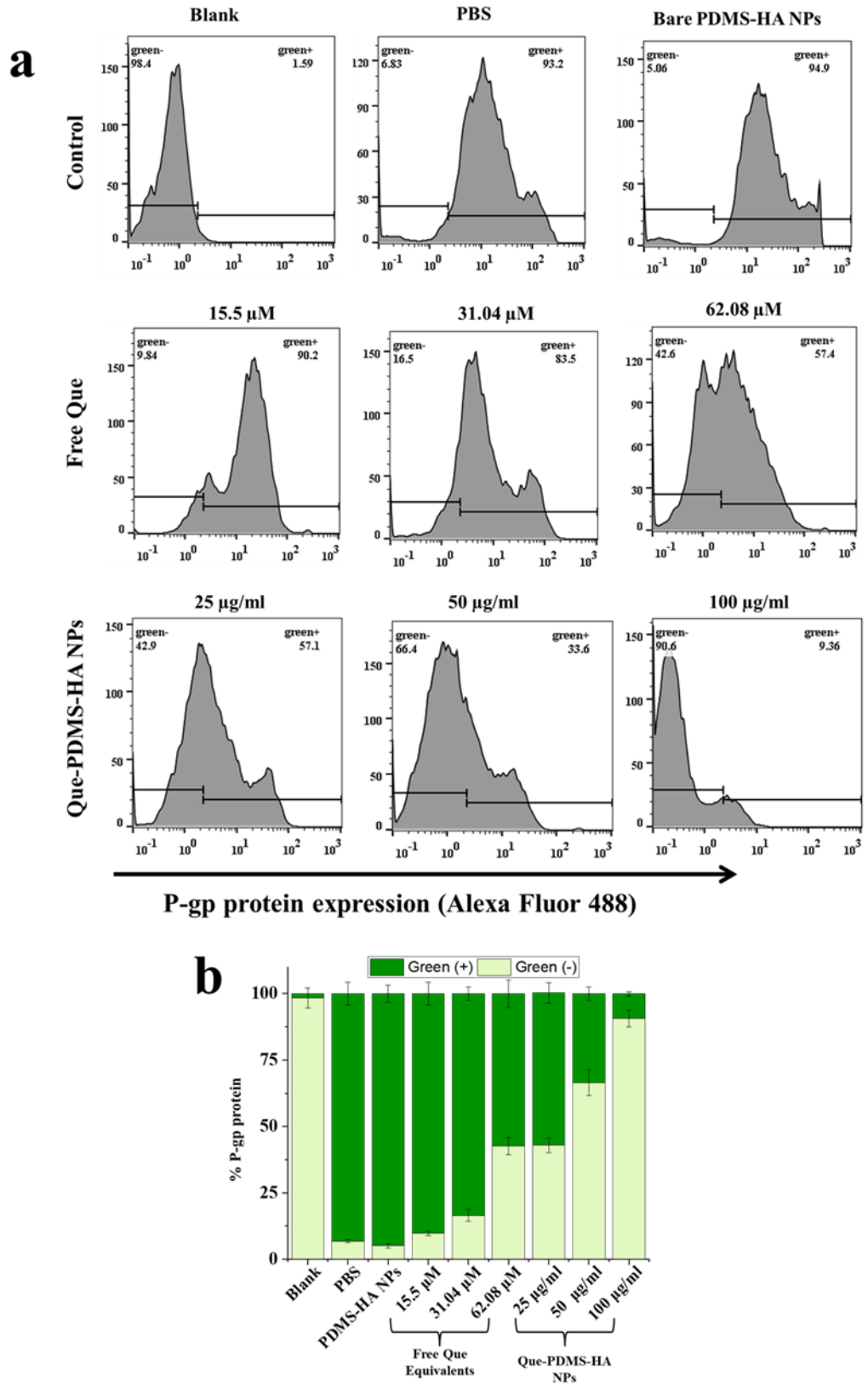

Fig. S13 Immunostaining studies of P-gp expression levels in MCF-7 cells. (a) Flow cytometry analysis of cells exposed to Que-PDMS-HA NPs and Free Que equivalents for 24h (b) Percentage of cells green(-), low expression of P-gp protein and green (+) high expression pf P-gp protein. Control groups include blank (no primary antibody, anti P-gp), PBS and bare PDMS-HA NPs. The results are represented as percentage green negative/positive cells (secondary antibody Alexa fluor 488).

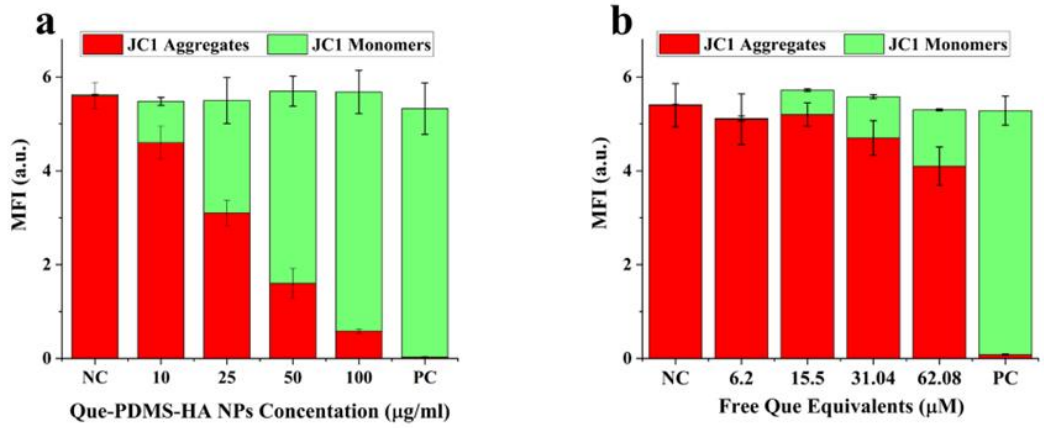

Fig. S14 The mean fluorescence intensity (MFI) quantification of JC-1 staining in MCF-7 cells treated with (a) Que-PDMS-HA NPs and (b) Free Que equivalents. Each data point signifies the average ± standard error (n = 3).

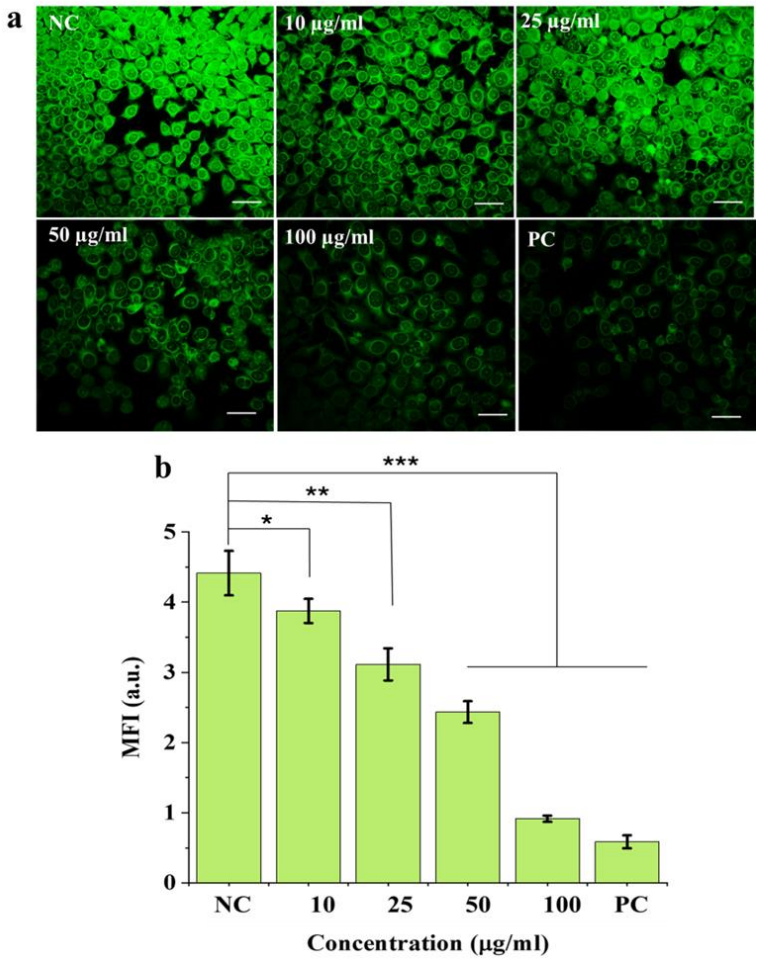

Fig. S15 Change in mitochondrial membrane potential in MCF-7 cells treated with Que-PDMS HA NPs (10, 25, 50, and 100), (a) confocal images, (b) MFI quantification of Rh123 dye. NC (untreated) PC (CCCP treated cells). Scale bar 20 µm. . (n=3, *$p < 0.05$,**$p < 0.01$ ***$p < 0.001$)

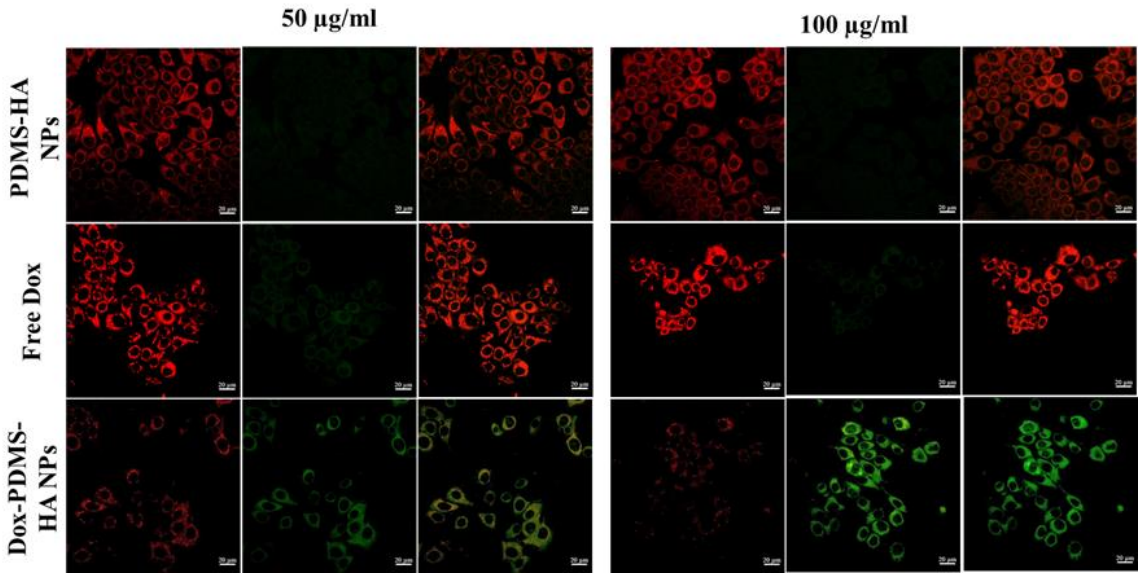

Fig S16. JC-1 assay for bare PDMS-HA NPs, free DOX and DOX-PDMS-HA NPs for 50 and 100 µg/ml and equivalent free Dox. Red (JC- 1 Aggregates) represents mitochondrial membrane potential intact and Green (JC-1 Monomers) represents mitochondrial membrane potential disrupted. Scale bar 20 µm.

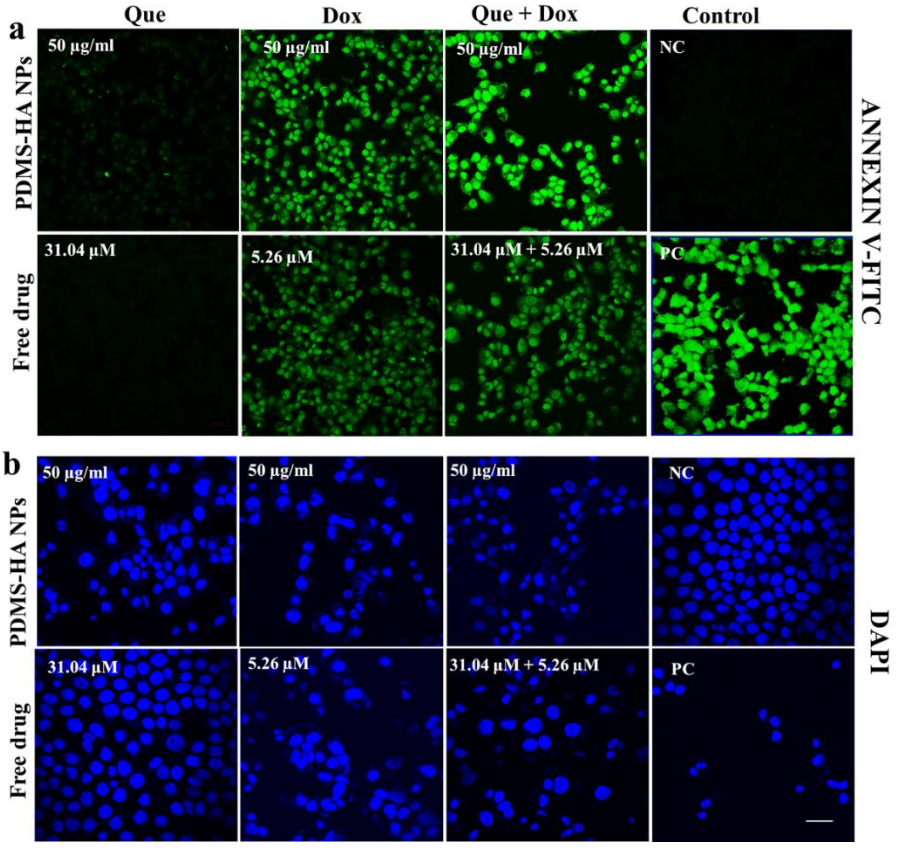

Fig. S17 Apoptosis assay analysis by (a) Annexin V-FITC and (b) DAPI staining. MCF-7 cells treated with Que-PDMS-HA NPs (50 µg/ml), Dox-PDMS-HA NPs (50 µg/ml), Que-Dox-PDMS-HA NPs (50 µg/ml), and their free equivalents for 24 h. NC: Negative control (PBS), and PC: positive control (H_2O_2 treated cells). Scale bar 50 µm.

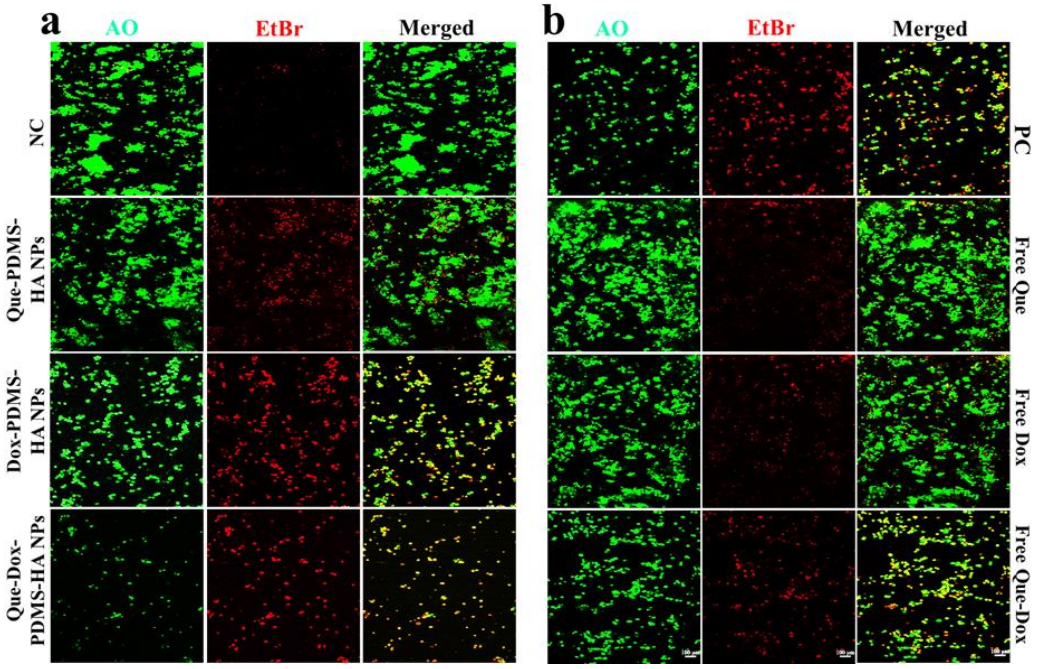

Fig. S18 AO/EtBr dual staining. (a) MCF-7 cells treated with 50 µg/ml of Que-PDMS-HA NPs, Dox-PDMS-HA NPs and Que-Dox-PDMS-HA NP, (b) free equivalents of Que and Dox. Scale bar 100µm

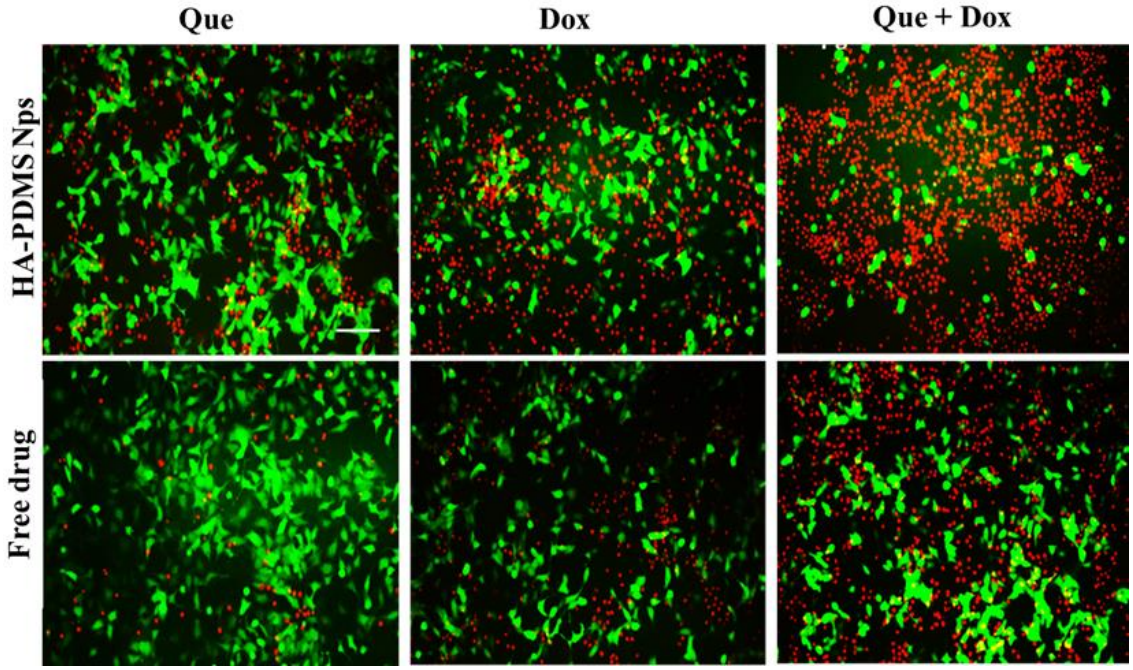

Fig. S19 Live dead analysis by FDA/PI staining. MCF-7 cells treated with 50 µg/ml of Que-PDMS-HA NPs, Dox-PDMS-HA NPs, Que-Dox-PDMS-HA NPs and their free equivalents for 24 h. Scale bar 50µm

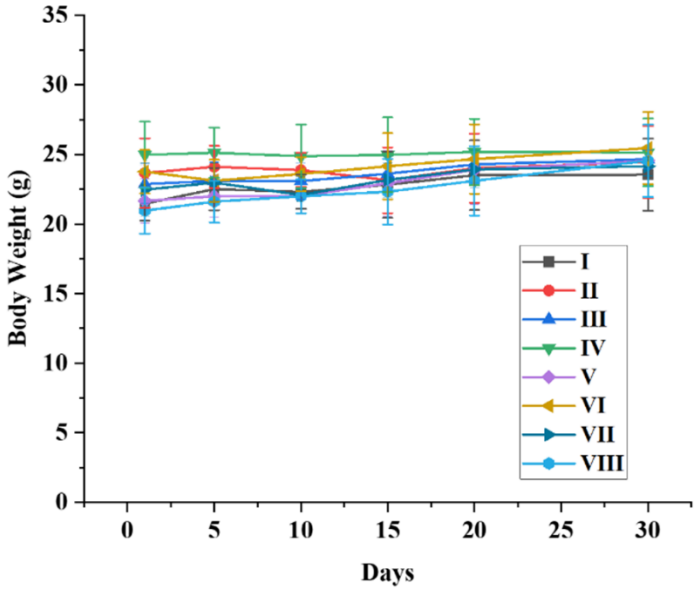

Fig. S20 Mice body weight Groups ((I) PBS, (II) Free Que, (III) Free Dox, (IV) Free Que+Dox, (V) bare-PDMS-HA NPs, (VI) Que-PDMS-HA NPs (VII), Dox-PDMS-HA NPs and (VIII) Que-Dox-PDMS-HA NPs). . Each data point signifies the average ± standard error (n = 4)

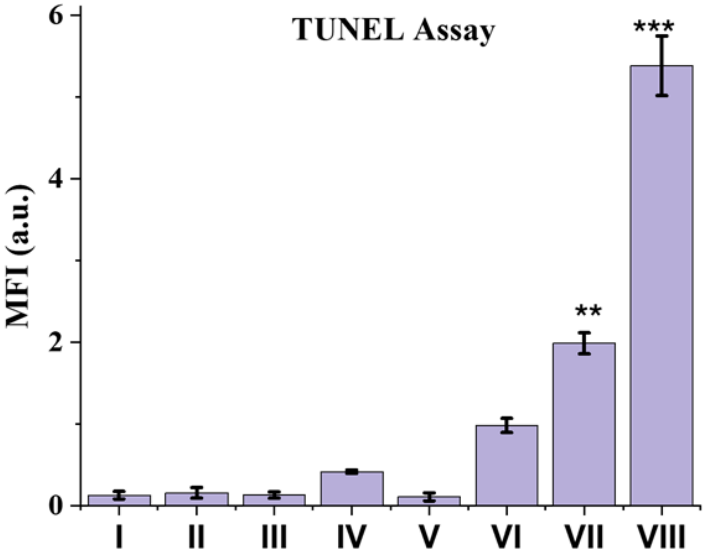

Fig. S21 The mean fluorescence intensity (MFI) quantification of the TUNEL assay for tumor sections Groups for the experiment: ((I) PBS, (II) Free Que, (III) Free Dox, (IV) Free Que+Dox, (V) bare-PDMS-HA NPs, (VI) Que-PDMS-HA NPs (VII), Dox-PDMS-HA NPs and (VIII) Que-Dox-PDMS-HA NPs). (**$p < 0.01$ ***$p < 0.001$)

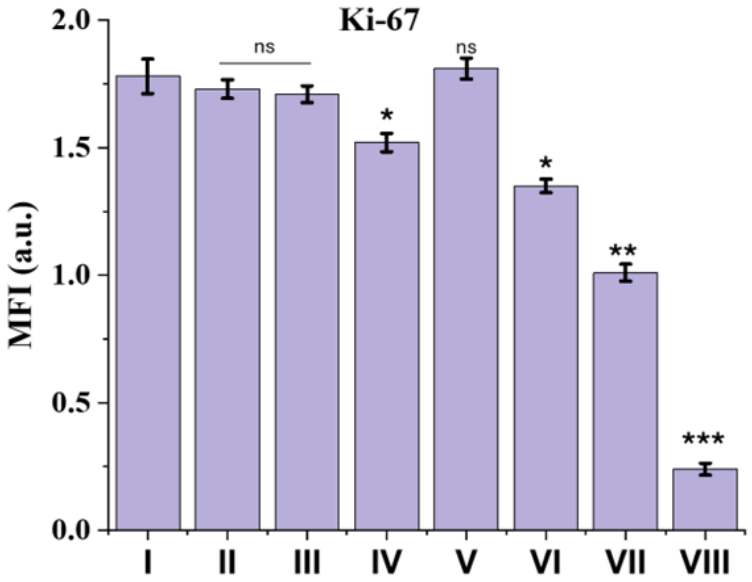

Fig. S22 The mean fluorescence intensity (MFI) quantification of the immunofluorescence (IHC) images for Ki67 expression in tumor sections Groups for the experiment: (((I) PBS, (II) Free Que, (III) Free Dox, (IV) Free Que-Dox, (V) bare-PDMS-HA NPs, (VI) Que-PDMS-HA NPs (VII), Dox-PDMS-HA NPs and (VIII) Que-Dox-PDMS-HA NPs). (*$p < 0.05$,**$p < 0.01$ ***$p < 0.001$).

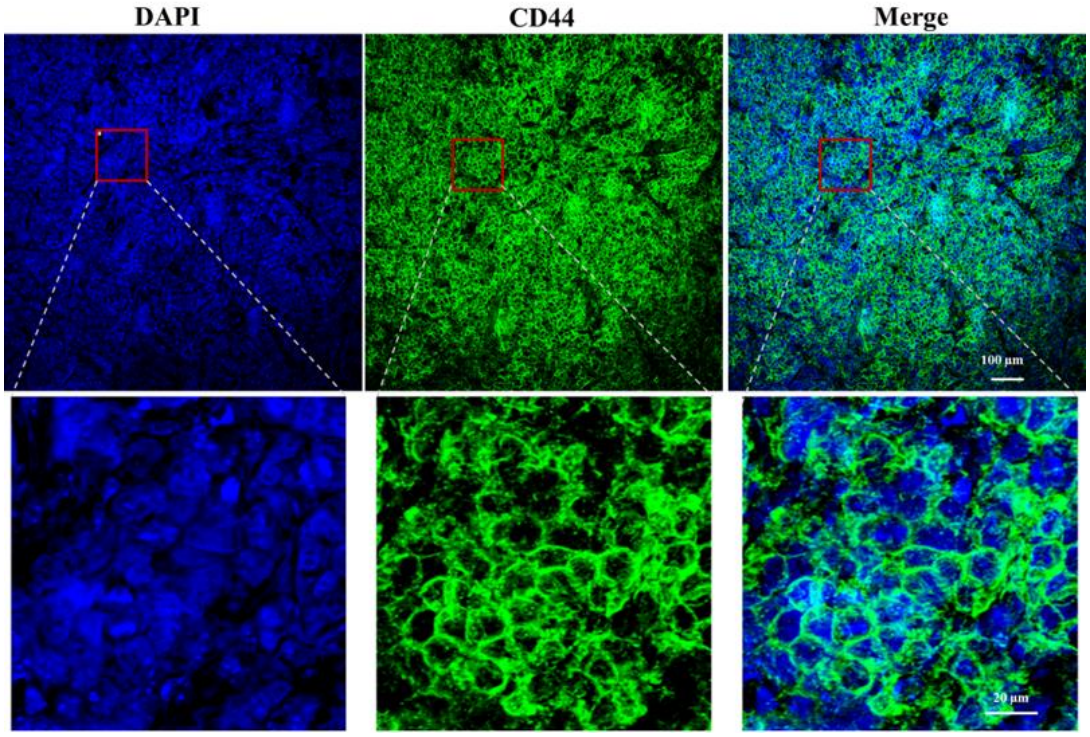

Fig. 23 IHC staining of MCF-7 xenograft tumor section with CD44 marker the green panel shows expression of CD44 in tumor cells, blue is nuclear stain DAPI . Scale bar 100µm and 20µm.

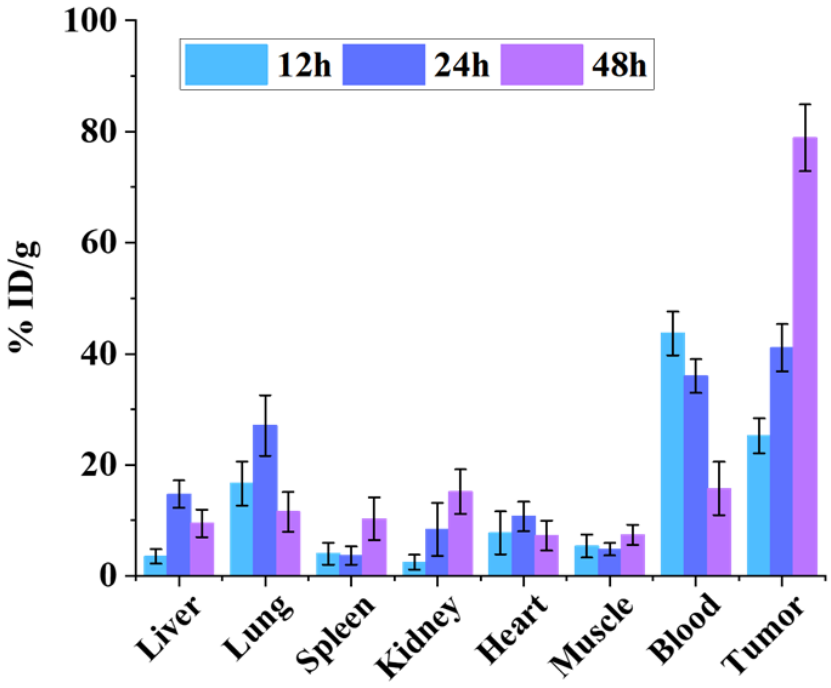

Fig. S24 Biodistribution analysis: ICP-MS measurement of Si amount in different organs and tumor. The mice bearing MCF-7 xenograft tumor were exposed to PDMS-HA NPs via IV dose. Organs were collected at different time points, and Si in ppb were measured through ICPMS. The Si amounts were determined as % of injected dose (ID). The results are shown as mean values ± SD

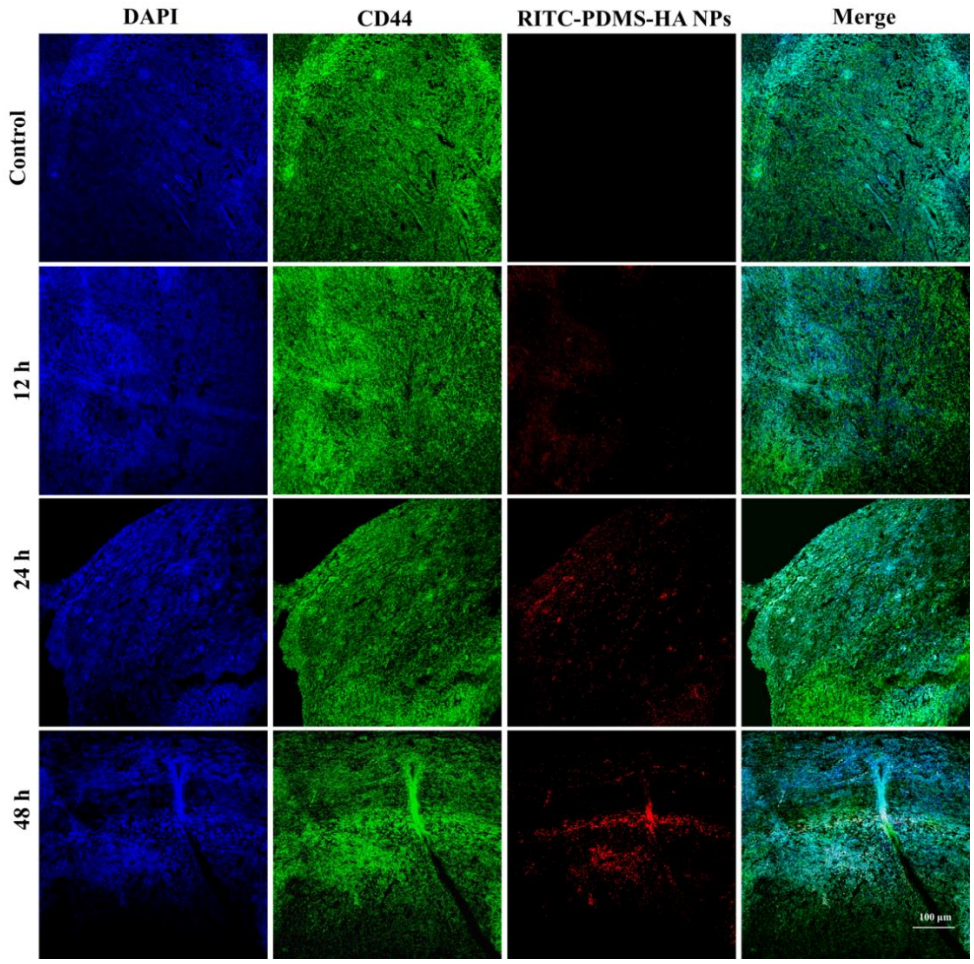

Fig. S25 IHC staining for tumor (MCF-7 xenografts) section with CD44 marker and RITC loaded HA-PDMS NPs. the green panel shows expression of CD44 in tumor cells, blue is nuclear stain DAPI, and the red panel shows the PDMS-HA NPs in the tumor sections. Scale bar 100µm.

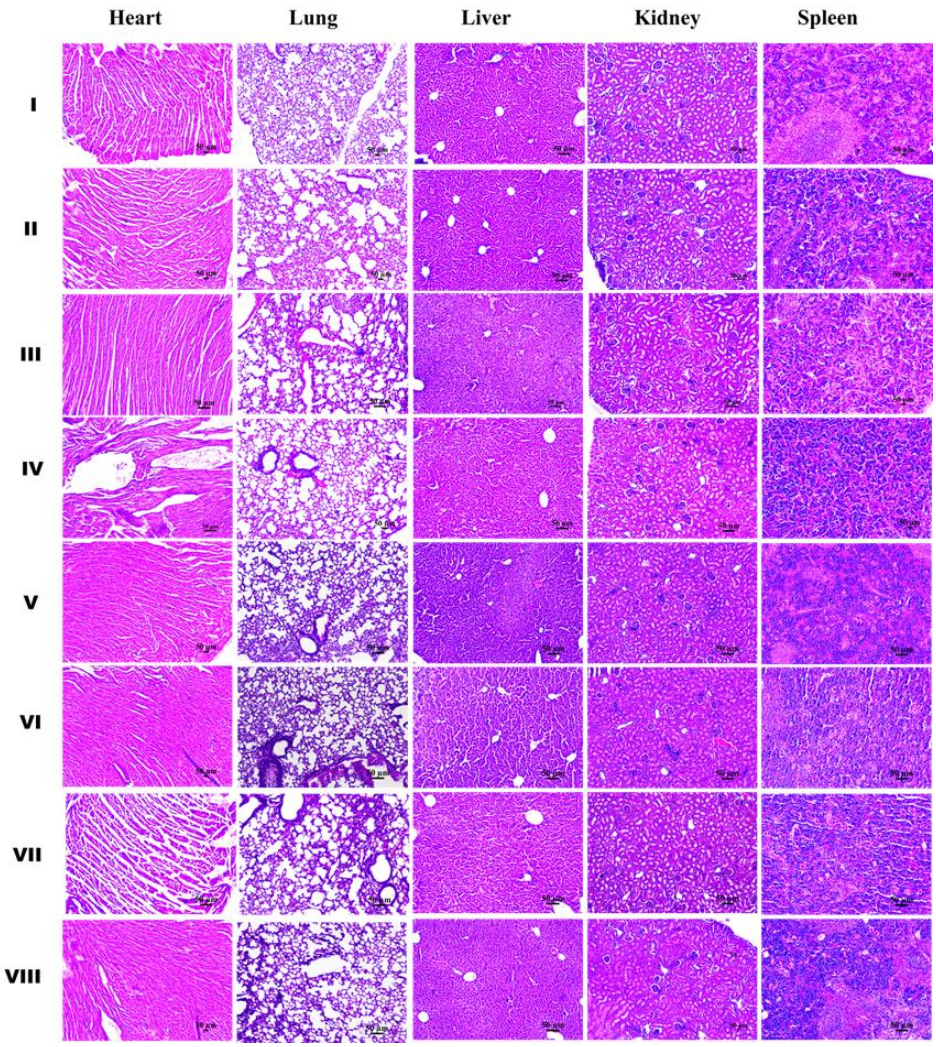

Fig. S26 Histological examination of various organs of tumor-bearing mice model treated with (I) PBS, (II) Bare-PDMS-HA NPs, (III) Free Que, (IV) Free Dox, (V) Free Que-Dox, (VI) Que-HA-PDMS NPs, (VII) Dox-PDMS-HA NPs, (VIII) Que-Dox-PDMS-HA NPs. Scale bar 50 μm.

References

1. Y. Hong, S. Che, B. Hui, X. Wang, X. Zhang and H. Ma, *Drug. Des. Devel. Ther.*, 2020, **14**, 2263–2274.
2. M. Liu, M. Fu, X. Yang, G. Jia, X. Shi, J. Ji, X. Liu and G. Zhai, *Colloids Surf. B Biointerfaces*, 2020, **196**, 111284.
3. S. Lev-Ari, H. Zinger, D. Kazanov, D. Yona, R. Ben-Yosef, A. Starr, A. Figer and N. Arber, *Biomed. Pharmacother*., 2005, **59**, S276–S280.
4. R. Wang, J. Huang, J. Chen, M. Yang, H. Wang, H. Qiao, Z. Chen, L. Hu, L. Di and J. Li, *Nanomedicine*, 2019, **21**, 102068.
5. Y. Wang, J. Ma, T. Qiu, M. Tang, X. Zhang and W. Dong, *Eur. J. Pharm. Sci*., 2021, **163**, 105864.
6. F.-L. Mi, L.-F. Wang, P.-Y. Chu, S.-L. Peng, C.-L. Feng, Y.-J. Lai, J.-N. Li and Y.-H. Lin, *ACS Biomater. Sci. Eng.*, 2018, **4**, 2847–2859.
7. Y. Zhang, C. Yang, W. Wang, J. Liu, Q. Liu, F. Huang, L. Chu, H. Gao, C. Li and D. Kong, *Sci. Rep.*, 2016, **6**, 21225.
8. J. Meng, F. Guo, H. Xu, W. Liang, C. Wang and X.-D. Yang, *Sci. Rep.*, 2016, **6**, 22390.
9. M. A. Vakilinezhad, A. Amini, T. Dara and S. Alipour, *Colloids Surf. B Biointerfaces*, 2019, **184**, 110515.
10. K. Jain, K. Thanki and S. Jain, *Mol. Pharm.*, 2013, **10**, 3459–3474.
11. Saneja, R. Kumar, M. J. Mintoo, R. D. Dubey, P. L. Sangwan, D. M. Mondhe, A. K. Panda and P. N. Gupta, *Mater. Sci. Eng. C*, 2019, **98**, 764–771.
12. P. Soltantabar, E. L. Calubaquib, E. Mostafavi, M. C. Biewer and M. C. Stefan, *Biomacromolecules*, 2020, **21**, 1427–1436.